Electronic Supplementary Material (ESI) for Nanoscale Advances.

Electronic Supporting Information

Microfluidic Schottky-Junction Photovoltaics with Superior Efficiency Stimulated by Plasmonic Nanoparticles and Streaming Potential

Mitradip Bhattacharjee,[a] Seim Timung,[b] Tapas Kumar Mandal[ab] and Dipankar Bandyopadhyay*[ab]

[a] *Centre for Nanotechnology, Indian Institute of Technology Guwahati, India*

[b] *Department of Chemical Engineering, Indian Institute of Technology Guwahati, India*

*Author to whom correspondences should be addressed. Email: dipban@iitg.ernet.in

I. Synthesis and Characterizations

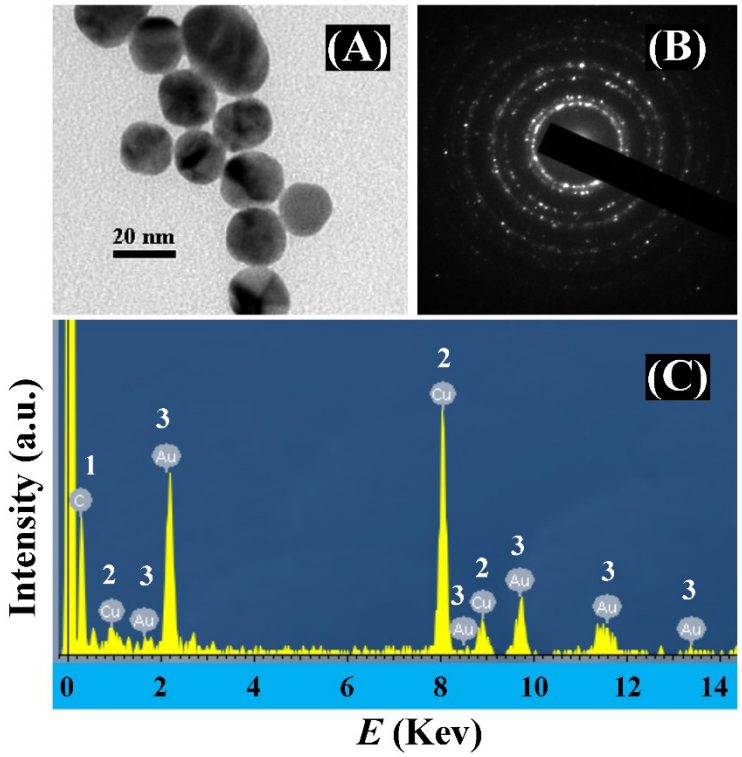

Figure S1: Image (A) shows the size and shape of the AuNPs from TEM. Image (B) shows the SAED pattern of synthesized AuNPs, and image (C) shows the EDX of the same. The numbers 1 to 3 in the image (c) represent the peaks of C, Cu, and Au, respectively.

The gold nanoparticles (AuNPs) were synthesized by reducing $HAuCl_4.3H_2O$.[1] Initially, we mixed $HAuCl_4.3H_2O$ with HCl in equal molar ratio, which resulted in a 50mM $AuCl^{4-}$ aqueous solution (solution I). Following this, $NaBH_4$ was dissolved in aqueous 1mM NaOH in equal molar ratio to prepare 50mM of BH^{4-} solution (solution II). Thereafter, a solution of 0.5mM gold ions was prepared by mixing 100 µl of solution I with water. Then, a 300 µl of solution II was mixed to the aqueous solution I with continuous stirring. The change in color of the solution from pale yellow to orange to red after few minutes of stirring indicated the formation of AuNPs. Transmission electron microscope (TEM) was performed for analyzing the size and shape of the AuNPs while energy dispersive X-ray spectroscopy (EDX) confirmed the presence of Au, as discussed in the **Figure S1**.

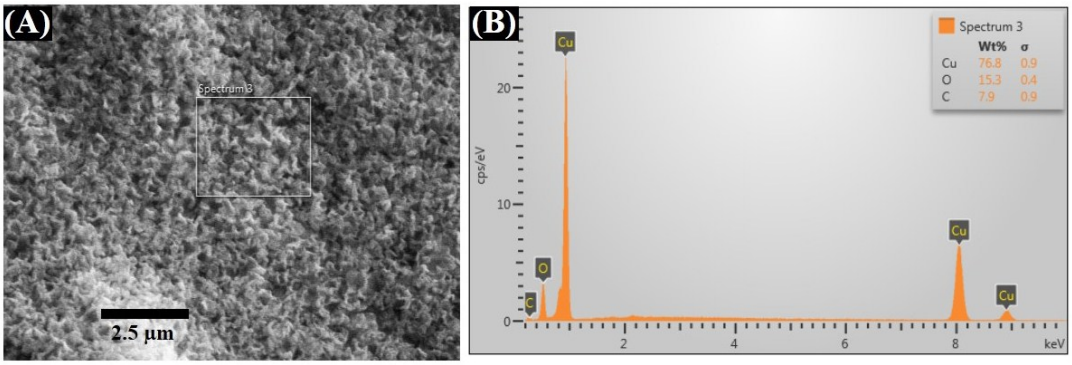

Figure S2: Image (A) shows the surface morphologies obtained from FESEM for the Cu_2O electrode and image (B) shows the EDX characterization of the same.

Copper (I) oxide (Cu_2O) was grown on Cu electrodes using thermal oxidation method where the cylindrical copper wire was heated for 30 s, 60 s, 80 s, and 90 s in presence of air. Consequently, copper (I) oxide formed on the surface of copper wires alongside forming a small amount of copper (II) oxide. The X-ray diffraction (XRD), Raman spectroscopy, and EDX confirmed the presence of copper oxides. Field emission scanning electron microscope (FESEM) was performed to examine the surface morphology of the electrodes. The FESEM and EDX images are shown in the **Figure S2** in which the image (A) shows the surface morphologies obtained from FESEM for the Cu_2O electrode and image (B) shows the EDX characterization confirming the presence of Cu_2O.

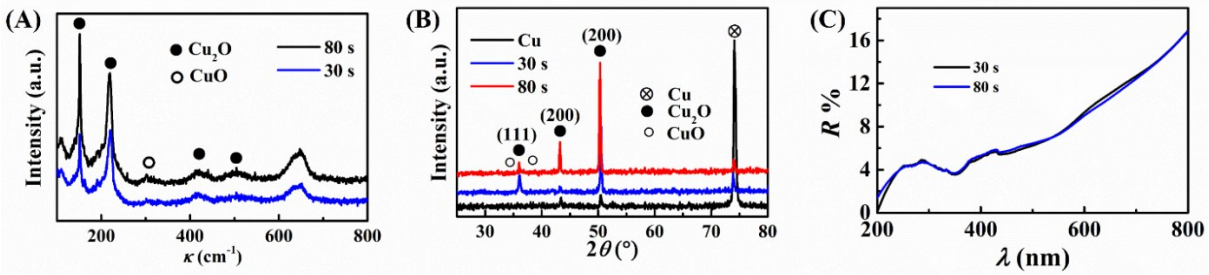

Figure S3. Images (A), (B), and (C) show the Raman spectroscopy, XRD, and UV-Vis spectroscopy characterizations, respectively, of the Cu_2O electrode at different time of heating.

The Cu_2O electrodes were characterized using Raman spectroscopy (514 nm laser excitation) and XRD, as shown in images (A) and (B), respectively, in the **Figure S3**. In both the analysis, we found characteristic peaks of Cu_2O with few small peaks of CuO.

Therefore, both Raman spectroscopy and XRD analysis confirmed successful growth of Cu_2O on electrode due to the controlled thermal oxidation of Cu. The optical property of the Cu_2O growth on the electrodes were further characterized with UV-Vis spectroscopy, as shown in **Figure 3(C),** in which the typical reflectance spectrum of Cu_2O electrode is plotted.

II. Microchannel fabrication and cleaning

Microwire moulding technique was employed to fabricate the microchannels.[2,3] Polydimethylsiloxane (PDMS - Dow Corning, Sylgard 184 kit) along with copper wire was used in this fabrication procedure. Copper wire of diameter ~300 μm were employed to construct the templates. The copper wires were joined by adhesives to get the required mould, which consisted of a main wire at the centre and a series of tributary wires, connected perpendicular to it. A trench of dimensions 50 mm × 30 mm × 5.5 mm (length × width × height) was prepared on a glass slide employing the double sided tapes. Thereafter, the prepared copper wire template was fit inside the trench. Then, a 1:10 (v/v) solution of cross-linker and pre-polymer of Sylgard 184 kit was prepared, which was degasified by keeping the solution in vacuum for 30 min. The solution was then dispensed on the trench and template. The trench with PDMS was then cured at 60^o C for 40 min in an air oven. After this, the PDMS was solidified and the cake was dipped in acetone to inflate and take out the copper wires. The resulting PDMS cake possessed one central microchannel connected to a series of tributary microchannels perpendicular to it, as shown in the **Figure 5(A).** The central main microchannel was fabricated for the electrolyte to flow in which one side of the same was used as the inlet for the salt-water flow and the other one as the outlet. The side microchannels were fabricated for electrode insertion and were integrated with the Cu-Cu_2O electrodes, as shown in the **Figure 5(B)**. All the microchannels had the inner diameter, d ~ 300 μm. Before the experiments initiated, the microchannels were cleaned for 10 min with acetone and methanol simultaneously in the ultra-sonic bath before cleaning with 10% (v/v) dilute piranha solution (H_2SO_4:H_2O_2, 3:1) for 15 min. Further, repeated washing of the microchannel was performed with DI water for 5 min. The microchannel was then dried by blowing

nitrogen gas followed by a heating of 20 min at 70°C in air-oven before used for the experiments.

III. Evaluation of Efficiency

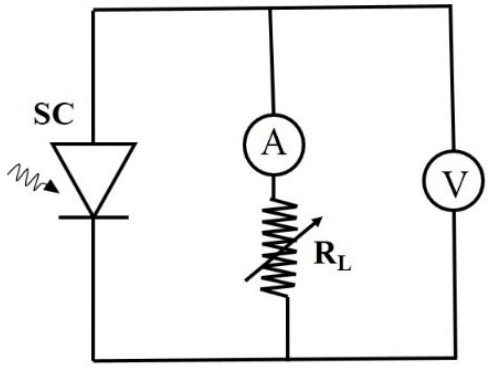

Figure S4: Circuit diagram for measuring the photo-current and photo-voltage characteristics of the DEH and MEH where SC is the DEH or MEH, which was connected to a voltmeter and an ammeter as shown. The notation R_L is a variable load resistance, which was tuned in order to get different set of photo-current and photo-voltage.

In order to evaluate the efficiencies, the power of the photo-illumination source (P_{in}) and the electrical power generated by the DEHs or MEHs were needed to be measured. The P_{in} was calculated from the ratio of the light intensity per unit area (I_0/A, lumen/m^2) to the luminous efficiency (lumen/W) of the source. For this purpose, the intensity per unit area of the light source was measured by a digital lux-meter and the luminous efficiency was obtained from the commercially available data-sheet of the light source. In order to measure the electrical power generated by the DEH or MEH, initially, the photo-current and photo-voltage characteristics were obtained. For this purpose, a variable resistance (R_L - range ~ 0 kΩ to 1 kΩ) was connected in series with the DEH or MEH. Following this, a voltmeter and an ammeter were integrated with the DEH or MEH in such a manner that the voltage and current could be measured across R_L, as shown in the **Figure S4**. For a given DEH or MEH, a set of current to voltage data were measured across the resistance, R_L, when its magnitude was varied from 0 to 1 kΩ. Thereafter, the current to voltage data were converted into a set of the power density data $(P = V \times J)$ corresponding to the DEH or MEH under consideration. Here P is the power generated by the DEH or MEH, V is the voltage and J is the corresponding current density. The current density data

required for the power calculation were obtained by dividing the current data with effective area of the electrodes (A_e) for energy harvesting. It may be noted here that the area of the top-half of the cylindrical electrodes (diameter ~240 μm and length ~150 μm), which was directly under the photo illumination was considered for the A_e calculation. The maximum electrical power density was obtained from the largest product of the current density to voltage data set, $(P_m = (V \times J)_m)$. Subsequently, the overall photo conversion efficiency was evaluated from the relationship,

$$\eta = \frac{P_m}{P_{in}}. \qquad (1)$$

One of important parameters to determine the electrical performance of any solar energy harvester is the fill-factor (*FF*), which is in general obtained from the following expression,

$$FF = \left(\frac{(V \times J)_m}{V_{OC} \times J_{SC}} \right) \times 100\%. \qquad (2)$$

Where V_{OC} and J_{SC} are the open-circuit voltage and short-circuit current density of the solar energy harvester. Thus, we also evaluated the *FF* for all the DEH and MEH reported in the present work. In order to evaluate V_{OC}, initially, the R_L was set to a very large value (e.g. ~1 kΩ), which ensured a negligible flow of current from DEH or MEH into the circuit (**Figure S4)** before measuring the voltage with the help of the voltmeter. In contrast, to evaluate J_{SC}, the R_L was set to a very small value (e.g. ~0 kΩ), which ensured a large flow of current from DEH or MEH into the circuit before measuring the current with the help of the ammeter. The experimentally determined values for V_{OC}, J_{SC}, and $(V \times J)_m$ were plugged into the Eq. (2) to obtain the *FF*.

IV. Effect of nanoparticles and optical characterization of AuNP

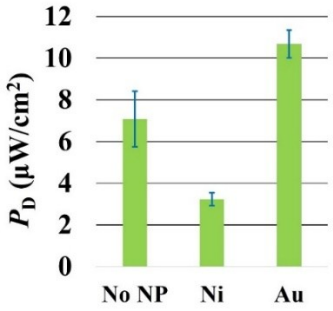

Figure S5: The image shows the power density of a 4M aqueous NaCl microdroplet with suspended gold nanoparticles (Au), nickel nanoparticles (Ni) nanoparticles, and without nanoparticles (NoNP) placed in between Cu and Cu2O electrodes exposed to a 100 W incandescent bulb at a luminous flux per unit area of 1.1 kLux.

Figure S5 shows the generation of power density in presence and absence of nanoparticles. A control experiment was performed where the Ni nanoparticles were suspended in a microdroplet and exposed to a light of intensity 1.1 kLux. The presence of Ni nanoparticels could not show any enhancement in the P_D whereas the AuNPs showed the enhancement due to the SPR effects.

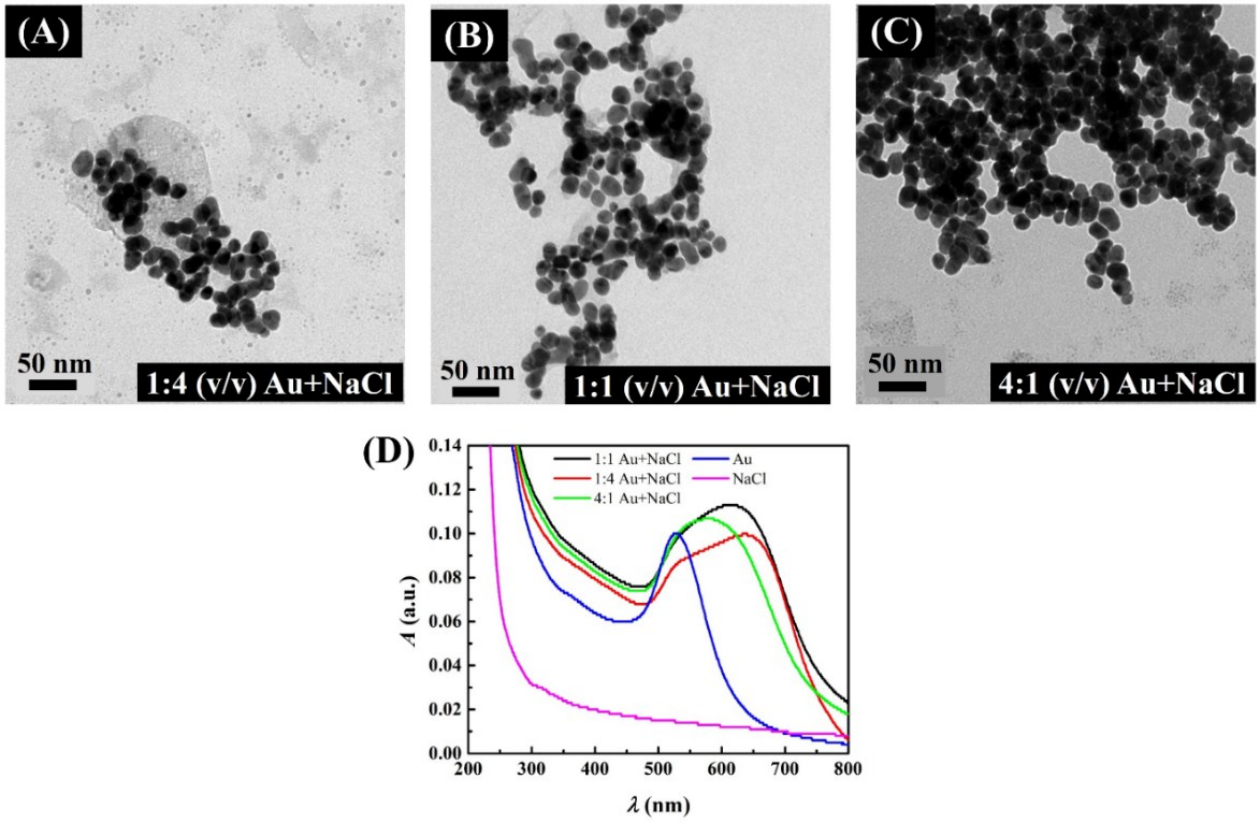

Figure S6: The TEM images of (A) 1:4 (v/v) (B) 1:1 (v/v) (C) 4:1 (v/v) AuNPs in 4M aqueous NaCl solution. Image (D) shows the UV-vis spectra for AuNP-NaCl mixture of different proportion (v/v).

Figure S6 illustrates the effect of electrolyte on the synthesized AuNPs. In this experiment, the synthesized AuNPs were mixed with 4M aqueous NaCl solution at different proportions (1:4, 1:1 and 4:1 v/v) before a TEM analysis was performed. It was found that the increase in the NaCl proportion led to higher agglomeration od AuNPs, as shown in the images (A – C). Moreover, the agglomeration of the AuNPs with the increase in its proportion in the aqueous salt solution had also been reflected in the enhanced absorption spectra, as illustrated through the UV-Vis spectroscopy image (D).

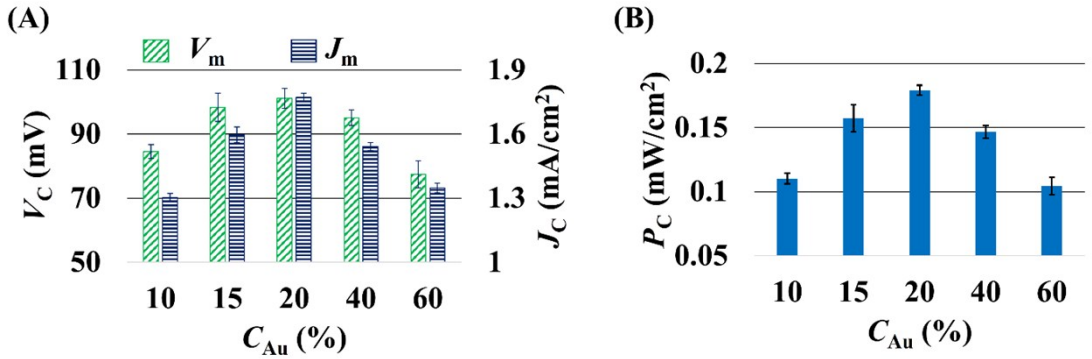

Figure S7: Image (A) shows the variation in generated voltage (V_C) and current density (J_C) with the AuNP loading (C_{Au}) for the 9-electrode MEH. Image (B) shows the variation in power density (P_C) with C_{Au} for the 9-electrode MEH. In all cases the light intensity was 1.1 kLux and F_R = 0.01 ml/min.

Figure S7 illustrates the performance of the effect of 9-electrode MEH. Image (A) shows the variation in potential difference generated (V_C) across the electrodes inside the channel and the subsequent current density (J_C) with the variation in the AuNP loading (C_{Au}) in the fluid. Image (B) shows the change in power density (P_C) across the electrodes inside the channel with C_{Au}. The plots suggest that the optimal loading for AuNPs was ~20% (v/v) for the MEH setup.

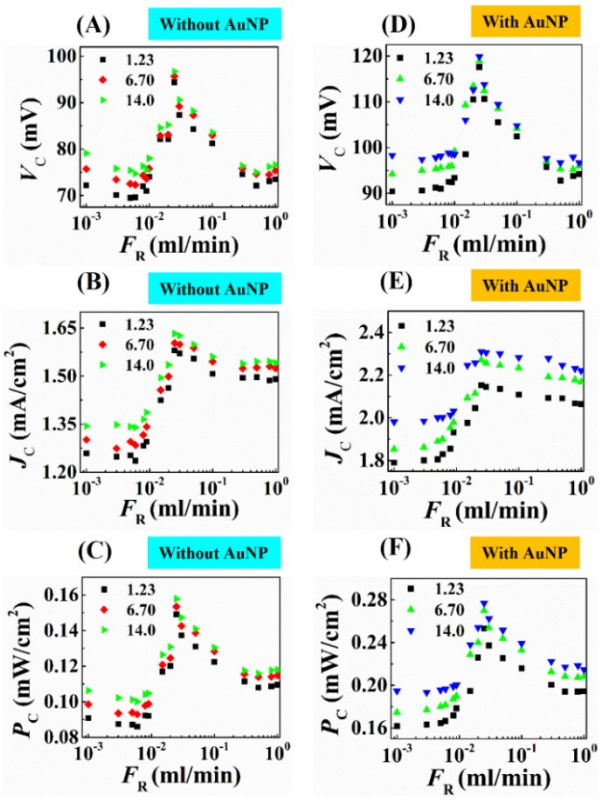

Figure S8: Images (A) – (C) [(D) – (F)] show the variations in the voltage generated (V_C), current density (J_C), and power density (P_C), respectively, with the flow rate (F_R) of the electrolyte 4M aq. NaCl solution [4M aq. NaCl solution with 20% (v/v) AuNPs] in the MEH-ECPV setup. The square, diamond, and triangle symbols on the images (A) – (F) represent light intensities of 1.23 kLux, 6.7 kLux, and 14 kLux, respectively.

Figures S8(A) – S8(C) show the variations in the voltage generated (V_C), current density (J_C), and power density (P_C), in the MEH with F_R when 4M aq. NaCl solution was flown. In these experiments, we inserted all 9-pair of electrodes for the experiments. The **Figures S8(D) – S8(F)** show similar plots as shown in the **Figures S8(A) – S8(C)** when the 4M aq. NaCl solution loaded with AuNPs [20% (v/v)] was flown.

V. Stability of the prototypes

Experiments were performed repeatedly with a single prototype for more than six months. The prototype was stable for at least six months. However, the electrodes show a stability of minimum of ~9 days with proper storage and cleaning with DI water after use. On the other hand, the organic, polymer, and perovskite solar cells suffers from environmental

stability which is less than a few hours in many a cases for organic and polymer solar cells in ambient conditions.[4]

VI. Supplementary Videos

Supporting Video S1 demonstrates an experiment in which a 4M aqueous NaCl microdroplet was dispensed in between a Cu and Cu_2O electrodes and then exposed to light source of 100 W incandescent bulb maintained at 4.5 kLux light intensity. In this case, a maximum of ~43 mV potential difference was observed between the electrodes.

Supporting Video S2 demonstrates the control experiment in which a 4M aqueous NaCl microdroplet was dispensed in between two Cu electrodes and then exposed to light source of 100 W incandescent bulb maintained at 4.5 kLux light intensity. In this case, no significant potential difference between the electrodes was observed.

Supporting Video S3 demonstrates an experiment in which a 4M aqueous NaCl microdroplet was initially loaded with AuNPs (4:1 v/v) before it was dispensed in between Cu and Cu_2O electrodes. The DEH shows the generation of ~90 mV under direct solar illumination, which amplified to ~114 mV using a bi-convex lens.

Supporting Video S4 demonstrates an experiment in which four 4M aqueous NaCl microdroplets were initially loaded with AuNPs (4:1 v/v) before they were dispensed in between Cu and Cu_2O electrodes. The DEH shows the generation of ~285 mV under direct solar illumination, which amplified to ~300 mV using a bi-convex lens.

Supporting Video S5 demonstrate an experiment of MEH in direct and focused solar illumination for 9-pairs of electrodes and 4M NaCl solution with AuNPs (4:1 v/v). The generated voltage was ~107 mV in direct solar illumination, which amplified to ~120 mV using bi-convex lens. The flow rate was maintained at 0.025 ml/min.

Supporting Video S6 demonstrate the application of the proposed system. An experiment was performed to turn on a LED. For this purpose, a DEH with 4M NaCl solution was connected to a LED through an amplifier circuit. The connected LED glowed upon illumination of 100 W incandescent bulb from a height of ~12.5 cm.

References:

1. M. N. Martin, J. I. Basham, P. Chando and S.-K. Eah, *Langmuir*, 2010, **26**, 7410-7417.
2. M. K. S. Verma, A. Majumder and A. Ghatak, *Langmuir* 2006, **22**, 10291–10295.
3. Y. Jia, J. Jiang, X. Ma, Y. Li, H. Huang, K. Cai, S. Cai and Y. Wu, *Chinese Sci. Bull.* 2008, **53**, 3928–3936.
4. D. Wang, M. Wright, N. Kumar, and E. A. Uddin, *Solar Energy Mat. Solar Cell.* 2016, **147**, 255-275